Int Ophthalmol
DOI 10.1007/s10792-015-0065-7

ORIGINAL PAPER

A novel Hartman Shack-based topography system: repeatability and agreement for corneal power with Scheimpflug+Placido topographer and rotating prism auto-keratorefractor

Gaurav Prakash · Dhruv Srivastava · Sounak Choudhuri

Received: 17 November 2014 / Accepted: 23 March 2015

Abstract The purpose of this study is to analyze the repeatability and agreement of corneal power using a new Hartman type topographer in comparison to Scheimpflug+Placido and autorefractor devices. In this cross sectional, observational study performed at the cornea services of a specialty hospital, 100 normal eyes (100 consecutive candidates) without any previous ocular surgery or morbidity except refractive error were evaluated. All candidates underwent three measurements each on a Full gradient, Hartman type topographer (FG) (iDesign, AMO), Scheimpflug+Placido topographer (SP) (Sirius, CSO) and rotating prism auto-keratorefractor (AR) (KR1, Nidek). The parameters assessed were flat keratometry (K1), steep keratometry (K2), steep axis (K2 axis), mean K, J_0 and J_{45}. Intra-device repeatability and inter-device agreement were evaluated. On repeatability analysis, the intra-device means were not significantly different (ANOVA, $p > 0.05$). Intraclass correlations (ICC) were >0.98 except for J_0 and J_{45}. In terms of intra-measurement standard deviation (Sw), the SP and FG groups fared better than AR group ($p < 0.001$, ANOVA). On Sw versus Average plots, no significantly predictive fit was seen ($p > 0.05$, $R^2 < 0.1$ for all the values). On inter-device agreement analysis, there was no difference in means (ANOVA, $p > 0.05$). ICC ranged from 0.92 to 0.99 ($p < 0.001$). Regression fits on Bland–Altman plots suggested no clinically significant effect of average values over difference in means. The repeatability of Hartman type topographer in normal eyes is comparable to SP combination device and better than AR. The agreement between the three devices is good. However, we recommend against interchanging these devices between follow-ups or pooling their data.

Keywords Hartman Shack topography · Full gradient topography · Scheimpflug topography · Auto keratorefractor · Repeatability

Introduction

Central keratometry plays a vital role in intraocular lens power calculation, refractive surgery, and other procedures dealing with corneal power. Assessment of corneal curvature is done by devices based on either the Scheiner principle, Placido rings, scanning slit method, scheimpflug photography, or a combination of these techniques [1, 2]. Multiple studies have compared these devices [3–6]. In general, the repeatability has been found to be satisfactory for most of these instruments; however, the agreement between devices has varied in studies [3–7].

In spite of being in clinical practice for a reasonably long time, most of these devices do have limitations. Keratometers measure only the central cornea, and

G. Prakash (✉) · D. Srivastava · S. Choudhuri
Department of Cornea and Refractive Surgery, NMC Eye Care, New Medical Center Specialty Hospital, Electra Street, PO Box 6222, Abu Dhabi, United Arab Emirates
e-mail: drgauravprakash@gmail.com

Published online: 28 March 2015

thus provide little information. Moreover, the corneal shape is assumed based on the preciseness of few rays reflected from predetermined points, rather than taking into account the actual corneal shape and its full gradient [8].

Placido ring based methods give much more information. However, they also have caveats. There is an ambiguity in determining corresponding points on the rings and the image, which may cause skew ray errors in reconstructing the corneal shape, especially in distorted corneas [9, 10]. Furthermore, adding a light source in the middle of the Placido rings leads to no actual capture from the central 2–4 mm, and thus the keratometry is extrapolated from the steepness of the area just outside this central area. This is based on specific assumptions on corneal asphericity and is therefore called 'simulated' keratometry, which can be inaccurate in cases with unexpected changes in corneal asphericity, such post-excimer ablation eyes [11].

Scheimpflug camera-based corneal assessment has been increasingly used in the recent past. Although the instruments based on rotating Scheimpflug cameras are considered more comprehensive and accurate, they have moving parts, and thus there is a possibility of inducing motion artifacts [12]. Moreover, radial scanning may not provide sufficient scan density of the corneal periphery which may further lead to the need for interpolation [12, 13].

Therefore, the ideal solution would be to capture true, detailed elevation data at each point of the central cornea, at high acquisition speeds without the use of a moving camera or paraxial approximation. Ray tracing (because it measures true deviation in the light rays) and swept-source optical coherence tomography (because of high speed of capture, leading to lesser motion artifact) have been suggested as newer alternatives [12, 13].

However, another useful approach is using a Hartman test-based method [8]. Hartman Shack principle has been used successfully for wavefront analysis. Results with prototype Hartman-based topographers on model surfaces and up to 5 human corneas in laboratory conditions have been published previously in feasibility studies [14, 15].

Recently, a new aberrometer, the iDesign advanced Wavescan studio (Abbott Medical Optics, Santa Ana, CA) has been launched for commercial use [8].

This device estimates corneal topography using a propriety, full gradient method based on the Hartman principle. As in wavefront aberrometry, the lenslets and grids are used to capture x and y slopes for each spot projected on the cornea [16]. The method, which has been described in further detail elsewhere, is briefly as follow: a cone-and-shell design is used to produce uniformly illuminated spots on the cornea. The cone, which faces the cornea, is perforated with holes that allow spots of light to be projected onto the eye. A shell behind the cone has a surface with Lambertian reflectance properties, producing uniform brightness at all angles. These spots are projected onto the cornea and the reflection is analyzed using pattern-recognition software. There is actual data capture from central 3-mm area and no extrapolation unlike in Placido rings method. Further, due to high acquisition speed and lack of moving parts, there are theoretically lesser chances of machine-related motion artifact and centration errors [16].

In this current study, we analyze the intra-user repeatability and agreement of keratometric and corneal astigmatism values in normal eyes using full gradient (FG) Hartman type topography (iDesign), Scheimpflug camera combined with Placido corneal (SP) topography [Sirius, Costruzione Strumenti Oftalmici (CSO), Italy], and rotating prism auto-keratorefractor (KR1, Topcon, Japan). The working of the Sirius device and the KR1 auto-keratorefractor have been described in detail elsewhere [7, 17].

To the best of our knowledge, this is the first study in published literature to evaluate the performance of Hartman shack-based topographer and compare it with other modern devices in a clinical setting.

Methods

This cross sectional, observation study was performed at the cornea and refractive surgery services of a tertiary care specialty hospital. Informed consents were obtained from all candidates. The study had the approval of the institutional review board and followed the tenets of the declaration of Helsinki. Cases included were young, normal candidates without any significant ocular morbidity other than refractive error. Cases with corneal scars, history of previous ocular surgery, and other ocular comorbidities were excluded. A total of 100 consecutive candidates were evaluated. All the scans were performed by an experienced examiner (DS) in dark room conditions. The three instruments were used in a random fashion using a three option random number sequence. A difference of 30 min was kept between examinations on the three instruments.

Method of Scheimpflug analysis

All the tests were done on the Sirius system. Patient's head was positioned on the chin rest and the topographer's height was adjusted until the centration cross was in the center of the rings. The patient was advised to blink a couple of times and then look straight into the fixation target. Then the image was focused with joystick control, maintaining the centration cross in the center of the Placido image and another cross sectional image of the cornea centered within the guidemarks. This was confirmed by color of the cross and by the guidemarks turning to from yellow to green in color. During the acquisition it was ensured that the cross and guidemarks remained centered and green. A good scan was denoted by a green tick in the acquisition quality icon. Three such consecutive good scans were taken for both eyes.

Method of Hartman type topography

All the tests were done on the iDesign system. After proper patient position, joystick controlled movements were used to achieve a good focus of the inbuilt grid. The patient was advised to blink a few times before the actual acquisition. After the acquisition, the captured data were analyzed by the instrument's inbuilt software for usable iris registration, wavefront data and corneal topography data. The review screen showed a green icon for all these three parameters when the measurements were usable. Three such consecutive good scans were taken for both eyes.

Method of autorefractor keratometry

The Topcon KR1 device was used. The patient was positioned with the forehead and chin aligned and supported. Eye height mark was aligned and the patient was asked to blink a couple of times. The pupil center as shown on the display touch screen was then tapped to automatically move the measuring head in correct position. The candidates were asked do look at the red-roof house (fixation target) during the acquisition. Three such good measurements were taken for both eyes.

Statistical analysis

One eye of each of the candidates was selected randomly using a binary option computerized random sequence generator. All the three measurements of the selected eye were used for repeatability analysis for each instrument (3 devices and 3 measurements each, total 9 measurements per evaluated parameter). Subsequently, one of the three measurements from each device was randomly selected using a three option random number sequence for analyzing the inter-device agreement.

The data were manually entered into a MS Excel (Microsoft, Richmond, VA). The data were then transferred to SPSS 16.0 (SPSS Inc., Illinois) for the analysis. K1 (flat keratometry), K1 axis, K2 (steep keratometry), K2 were taken directly from the instruments' outputs. The mean K (arithmetic mean of K1 and K2), corneal cylinder (K1–K2, negative cylinder notation), primary astigmatism (J_0), and oblique astigmatism (J_{45}) were computed.

The corneal astigmatism was converted into vector representation, J_0 and J_{45}, which were calculated as follows: [18].

$$J_0 = -[\text{cylinder}/2]\cos[2 \times \text{axis}]$$

$$J_{45} = -[\text{cylinder}/2]\sin[2 \times \text{axis}].$$

Intra-device repeatability

Intra-device repeatability was analyzed for all the three instruments initially. Analysis of variance (ANOVA) was used to evaluate the difference in means. Intra-measurement standard deviation (Sw) and its related parameters, precision (1.96 × Sw), and repeatability (2.77 × Sw) were computed [19].

Intraclass correlations (two-way mixed, for absolute measures, and showing average value) were computed for intra-device repeatability. Finally, the intra-measurement standard deviation was plotted as a function of the average value [x, $y \rightarrow$ average of (M1, M2, M3), Sw], where M1, M2, and M3 are the values noted on the three measurements.

Inter-device agreement

Analysis of variance (ANOVA) was used to analyze the difference of mean. Tukey's post HOC test was used for comparing the subgroups. Intraclass correlations were computed (two-way mixed method, absolute agreement and showing average values). Best fit regression plots were plotted to see the fits between same variables from two different instruments at a time. Bland–Altman plot were drawn to plot the difference between values and their averages for two instruments at a time.

Table 1 Outcomes of intra-device repeatability

Variable[a]	Device[b]	Mean 1[c]	Mean 2[c]	Mean 3[c]	pooled mean[d]	Pooled SD[d]	Sw	Precision	Repeatability	Coefficent of variation	ICC
Flat keratometry	S+P	42.52	42.47	42.51	42.50	1.53	0.14	0.28	0.40	0.34	0.996
	FG	42.51	42.51	42.53	42.51	1.51	0.14	0.28	0.40	0.34	0.996
	AR	42.51	42.54	42.45	42.50	1.48	0.26	0.50	0.71	0.60	0.988
Steep keratometry	S+P	43.65	43.67	43.64	43.66	1.60	0.16	0.31	0.44	0.36	0.996
	FG	43.63	43.62	43.66	43.64	1.53	0.17	0.33	0.47	0.38	0.995
	AR	43.56	43.57	43.62	43.58	1.55	0.30	0.59	0.83	0.69	0.985
Axis of steep keratometry	S+P	92.35	91.92	92.79	92.35	22.65	2.37	4.64	6.56	2.56	0.995
	FG	91.50	91.37	90.92	91.26	24.35	2.19	4.30	6.07	2.40	0.997
	AR	90.66	90.08	90.08	90.27	23.32	3.18	6.23	8.80	3.52	0.993
Mean keratometry[e]	S+P	43.08	43.07	43.07	43.08	1.52	0.10	0.20	0.28	0.23	0.997
	FG	43.07	43.06	43.10	43.08	1.46	0.10	0.19	0.27	0.23	0.998
	AR	43.03	43.06	43.03	43.04	1.45	0.18	0.36	0.50	0.42	0.993
J_0	S+P	−0.502	−0.530	−0.499	−0.510	0.422	0.100	0.20	0.28	–	0.974
	FG	−0.478	−0.473	−0.477	−0.476	0.438	0.098	0.19	0.27	–	0.976
	AR	−0.469	−0.456	−0.502	−0.476	0.437	0.175	0.34	0.48	–	0.922
J_{45}	S+P	−0.022	−0.016	−0.012	−0.016	0.239	0.064	0.12	0.18	–	0.972
	FG	−0.022	−0.025	−0.031	−0.026	0.261	0.069	0.13	0.19	–	0.968
	AR	−0.053	−0.050	−0.081	−0.061	0.264	0.101	0.20	0.28	–	0.909

Sw: intra-measurement standard deviation ($n = 3$). Precision: 1.96 × Sw; Reliability: 2.77 × Sw

Coefficient of Variation expressed as percentage, not computed for variables that had both the negative and positive values

ICC computed as two-way mixed, for absolute agreement and using average measures

p value <0.001 for all ICC values

[a] All values for descriptive data are in dioptres except for axis of steep keratometry (degrees)

[b] Device: S+P: Scheimpflug+Placido (Sirius); *FG* Full Gradient, Hartman topographer (iDesign); *AR* Auto kerato-refractor (KR1)

[c] Pooled mean and Pooled SD: overall mean and standard deviation of the variable for each device ($n = 300$)

[d] Means for the measurement # 1, 2, and 3 for each instrument ($n = 100$ each). p value >0.05 for all comparison between measurements # 1, 2, 3 for ANOVA test

[e] Mean keratometry: arithmetic average of steep and flat keratometry

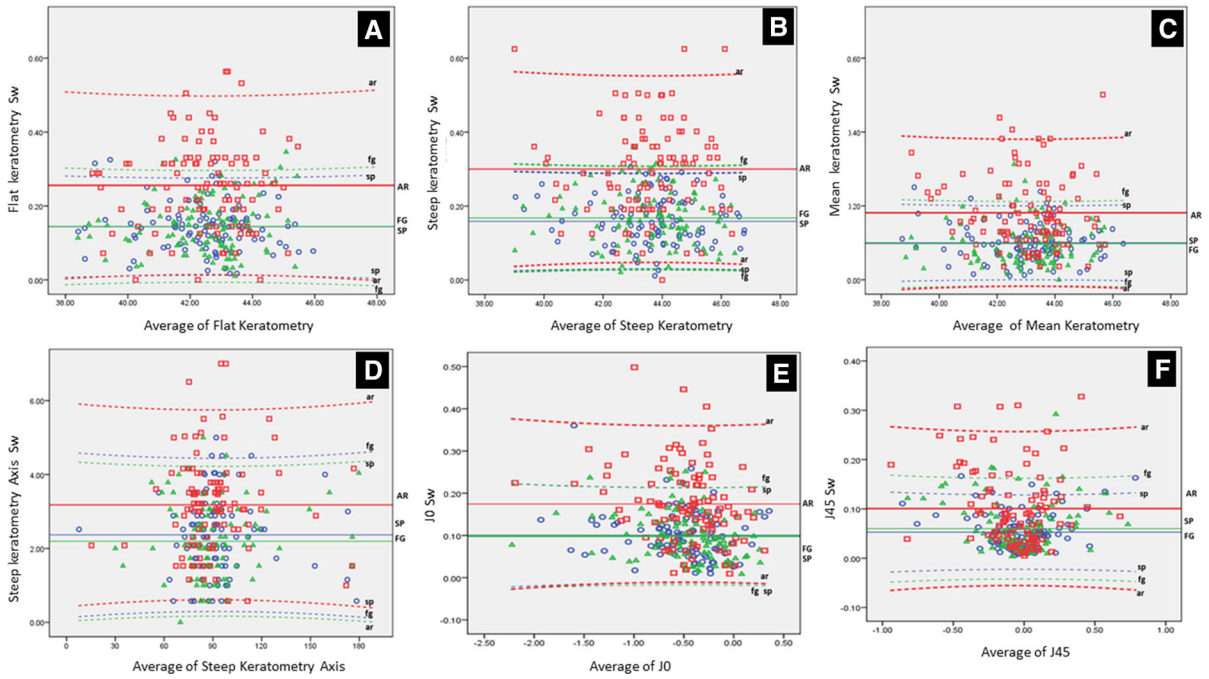

Fig. 1 Overall scattergrams for repeatability analysis for the three devices [Autorefractor (AR), Scheimpflug+Placido (SP), and Hartmann type full gradient topographer (FG)]. Intra-measurement standard deviation (Sw) is plotted as a function of average value. The *red squares* denote AR, *blue circles* SP, and *green triangles* FG. The uppercase acronyms (AR, FG and SP) are used to label mean Sw, denoted by solid lines and the lowercase acronyms (ar, fg and sp) are used to label 95 % confidence interval limits of the data, denoted by dashed lines. **a** Flat keratometry; **b** Steep keratometry; **c** Mean keratometry; **d** Steep keratometry axis; **e** J_0, and **f** J_{45}

Results

Demography

There were 56 males and 44 females. The right eye was randomly selected in 47 cases and the left eye in remaining 53 cases. The mean age was 26.4 ± 4.9 years.

Analysis for intra-device repeatability

Means, descriptive statistics, and measures for repeatability

The mean values for each measurement, the pooled mean and standard deviation (SD), intra-measurement standard deviation (Sw), its derived statistics, precision and repeatability, and the interclass correlations (ICC) have been tabulated in Table 1. ICCs were >0.98 except for J_0 and J_{45}. Coefficients of variation were low (<0.7) for all keratometric measurements. However, the coefficient of variation ranged between 2.4 and 3.5 for the steep axis. Even though all the values for repeatability measures were low and clinically acceptable, the SP and FG groups fared better statistically compared to the AR group in terms of intra-measurement standard deviation. On metadata analysis, Sw were found to be significantly better for the SP and FG groups in comparison to AR group ($p < 0.001$ for all the 6 variables between mean Sw from S+P, FG and AR, ANOVA). This was seen in spite the three groups being comparable in terms of intra-measurement heterogeneity ($p > 0.05$ for all variables between mean values of three measures each from SP, FG and AR, ANOVA).

Sw plots

Overlay Sw versus average plots were drawn. The 95 % confidence interval of the data was shown along with the mean Sw (Fig. 1). The 95 % confidence intervals were generally greater for AR compared to the other two devices. There was no significantly predictive fit between Sw and Average value for all the 6 data sets ($p > 0.05$, $R^2 < 0.1$ for all the values).

Table 2 Descriptive statistics for the three sets of data used for inter-device agreement

		N	Mean	Standard deviation	Minimum	Maximum
Flat keratometry (D)	S+P	100	42.52	1.52	38.56	45.90
	FG	100	42.52	1.49	38.53	45.35
	AR	100	42.49	1.45	38.70	45.25
	Total	300	42.51	1.48	38.53	45.90
Steep keratometry (D)	S+P	100	43.65	1.61	38.98	46.93
	FG	100	43.61	1.52	38.93	46.54
	AR	100	43.60	1.54	39.00	46.49
	Total	300	43.62	1.55	38.93	46.93
Steep axis (degrees)	S+P	100	92.50	22.40	10.00	178.00
	FG	100	91.30	24.23	28.00	179.00
	AR	100	90.14	23.27	13.00	178.00
	Total	300	91.31	23.26	10.00	179.00
Average keratometry (D) (Steep + Flat)/2	S+P	100	43.09	1.52	38.77	46.26
	FG	100	43.06	1.45	38.82	45.62
	AR	100	43.04	1.45	38.88	45.62
	Total	300	43.06	1.47	38.77	46.26
J_0 (D)	S+P	100	−0.50	0.41	−1.98	0.32
	FG	100	−0.46	0.43	−2.24	0.33
	AR	100	−0.49	0.39	−1.96	0.34
	Total	300	−0.48	0.41	−2.24	0.34
J_{45} (D)	S+P	100	−0.02	0.22	−0.92	0.68
	FG	100	−0.03	0.23	−0.77	0.73
	AR	100	−0.06	0.24	−0.79	0.59
	Total	300	−0.04	0.23	−0.92	0.73

S+P Scheimpflug+Placido topographer, *FG* full gradient, Hartman type topographer, *AR* rotating prism auto keratorefractor

Analysis for inter-device agreement

Measures of central tendency and repeatability

The mean, standard deviation, and other descriptive data of flap keratometry (K1), steep keratometry (K2), axis of steepest cornea (K2 axis), the mean keratometry and J_0 and J_{45} have been given in Table 2. There was no difference in the means of all the compared variables as a group (ANOVA, $p > 0.05$, Table 3), and on subgroup comparisons (Tukey's post hoc test, $p > 0.05$, Table 3).There was highly significant correlation between the three devices (Table 3) with r ranging for Pearson's correlation from 0.92 to 0.99 ($p < 0.001$) for all measured variables except J_{45} ($r = 0.75$–0.87, $p < 0.001$). The best results for correlation were seen with steep keratometry, flat keratometry, and the mean keratometry. Intraclass correlations were computed to look at the absolute agreement between the variables from the three devices. High ICC values were seen for all parameters (0.92–0.99, $p < 0.001$, Table 3).

Best fit regression curves

Best fit curves were plotted with the R^2 statistics ranging from 0.97 to 0.57 ($p < 0.001$ for all comparisons) for as seen in Figs. 2, 3 and 4. All the parameters other than J_{45} had a R^2 of ≤ 0.85 for the linear best fit.

Bland–Altman plots

The difference of mean and 95 % limits of agreements were computed and drawn in the Bland–Altman plots. None of the best fit lines in the bland–Altman curves had a strong predictive fit (all $R^2 < 0.06$ and p values > 0.05 for most variables). Only best fit lines for AR

Table 3 Difference in means, ANOVA and correlation statistics for inter-device agreement

Dependent variable	ANOVA (p value)	Subgroup analysis Tukey's test						Correlations	
		(*I*) Group[a]	(*J*) Group[a]	Mean difference (I–J)	Sig.	95 % CI[b] lower	95 % CI[b] upper	Pearson correlation*	ICC
Steepest keratometry (D)	0.9	S+P	FG	0.01	0.99	−0.49	0.50	0.98	0.99
		S+P	AR	0.04	0.98	−0.46	0.53	0.97	
		FG	AR	0.03	0.99	−0.47	0.53	0.99	
Flattest keratometry (D)	0.9	S+P	FG	0.05	0.97	−0.47	0.57	0.97	0.99
		S+P	AR	0.05	0.97	−0.47	0.57	0.96	
		FG	AR	0.00	0.99	−0.52	0.52	0.99	
Steepest keratometry axis (degree)	0.8	S+P	FG	1.20	0.93	−6.57	8.97	0.92	0.97
		S+P	AR	2.36	0.75	−5.41	10.13	0.93	
		FG	AR	1.16	0.93	−6.61	8.93	0.93	
Astigmatism (D)	0.9	S+P	FG	0.04	0.92	−0.21	0.30	0.92	0.97
		S+P	AR	0.01	0.99	−0.24	0.27	0.92	
		FG	AR	−0.03	0.96	−0.28	0.23	0.92	
Average keratometry (D)	0.9	S+P	FG	0.03	0.99	−0.46	0.52	0.98	0.99
		S+P	AR	0.04	0.98	−0.45	0.54	0.97	
		FG	AR	0.02	0.99	−0.47	0.51	0.99	
J_0 (D)	0.8	S+P	FG	−0.04	0.78	−0.17	0.10	0.93	0.97
		S+P	AR	−0.02	0.96	−0.15	0.12	0.93	
		FG	AR	0.02	0.92	−0.11	0.16	0.92	
J_{45} (D)	0.3	S+P	FG	0.01	0.97	−0.07	0.08	0.87	0.92
		S+P	AR	0.05	0.35	−0.03	0.12	0.79	
		FG	AR	0.04	0.49	−0.04	0.11	0.75	

[a] *FG* Full Gradient topography, S+P: Scheimpflug plus Placido, *AR* Autorefractor with rotating prism

[b] *CI* Confidence interval

* Pearson Correlation: all the p values were <0.001

[#] *ICC* Intraclass correlation between the three devices for the measured variable. Computed for absolute agreement (Two way mixed, absolute agreement). All ICC had p value <0.001

versus SP for flat keratometry ($p = 0.04$, $R^2 = 0.04$), SP versus FG for mean keratometry ($p = 0.04$, $R^2 = 0.04$), and AR versus FG for J_0 ($p = 0.02$, $R^2 = 0.06$) had p values more than 0.05. However, the R^2 for these comparisons were low, suggesting no clinically important effect of the increase or decrease in the magnitude of studied parameter on the difference achieved between (Figs. 5, 6, 7).

Discussion

Central keratometry plays a vital role in intraocular lens power calculation, refractive surgery and other procedures dealing with corneal power. The combined usage of Scheimpflug imaging and Placido technology in the Sirius topographer gives it the unique advantage of both the existing technologies. On the other hand, autorefractor based assessment of the corneal power has been used for a long time, especially in intraocular lens power calculation and contact lens fitting. Therefore, we decided to compare the outcomes of these two devices with the new device, the full gradient, Hartman type topographer (iDesign).

All the three devices had excellent repeatability, which was well within the clinically acceptable ranges. The ICC and Sw seen with Sirius in our study were comparable to those reported earlier [7, 20]. There are no similar studies in the literature for iDesign and KR1 specifically.

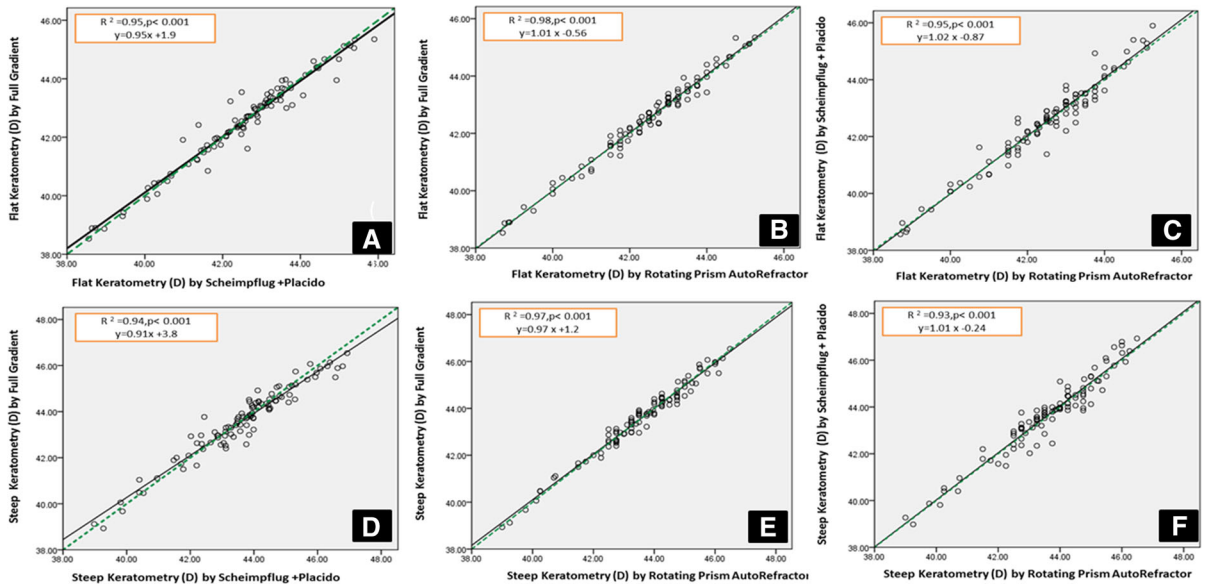

Fig. 2 Best fit linear plots between the same variable derived from two different devices [Autorefractor (AR), Scheimpflug+Placido (SP), and Hartmann type full gradient topographer (FG)] for the same patient. The *dashed green line* is the line of equivalence ($y = x$) and the *solid black line* is that of the best fit linear equation. **a** flat keratometry for FG versus SP; **b** flat keratometry for FG versus AR; **c** flat keratometry for SP versus AR; **d** steep keratometry for FG versus SP; **e** steep keratometry for FG versus AR; **f** steep keratometry for SP versus AR

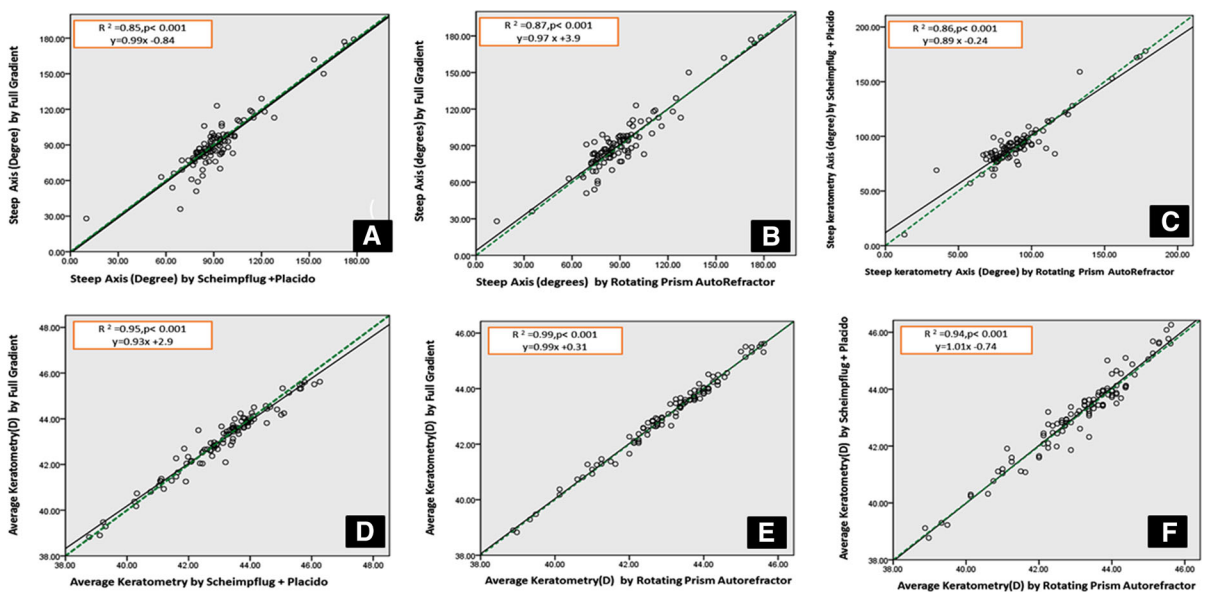

Fig. 3 Best fit linear plots between the same variable derived from two different devices [Autorefractor (AR), Scheimpflug+Placido (SP), and Hartmann type full gradient topographer (FG)] for the same patient. The *dashed green line* is the line of equivalence ($y = x$) and the *solid black line* is that of the best fit linear equation. **a** steep keratometry axis for FG versus SP; **b** steep keratometry axis for FG versus AR; **c** steep keratometry axis for SP versus AR; **d** average keratometry for FG versus SP; **e** average keratometry for FG versus AR; **f** average keratometry for SP versus AR

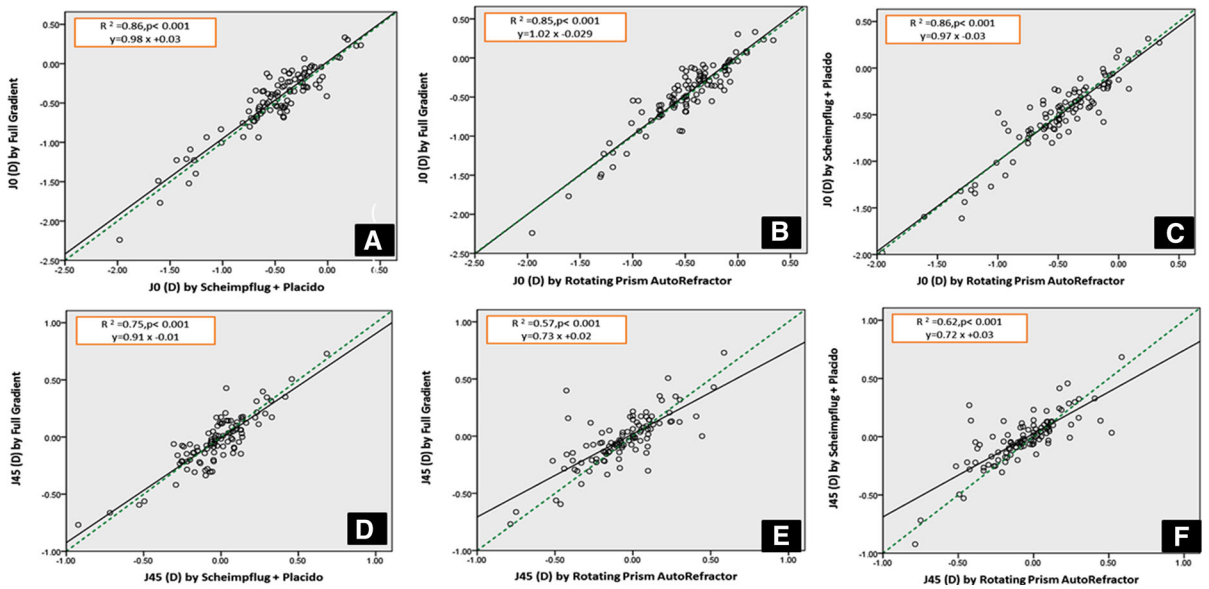

Fig. 4 Best fit linear plots between the same variable derived from two different devices [Autorefractor (AR), Scheimpflug+Placido (SP) and Hartmann type full gradient topographer (FG)].The *dashed green line* is the line of equivalence ($y = x$) and the *solid black line* is that of the best fit linear equation. **a** J_0 for FG versus SP; **b** J_0 for FG versus AR; **c** J_0 for SP versus AR; **d** J_{45} for FG versus SP; **e** J_{45} for FG versus AR; **f** J_{45} for SP versus AR

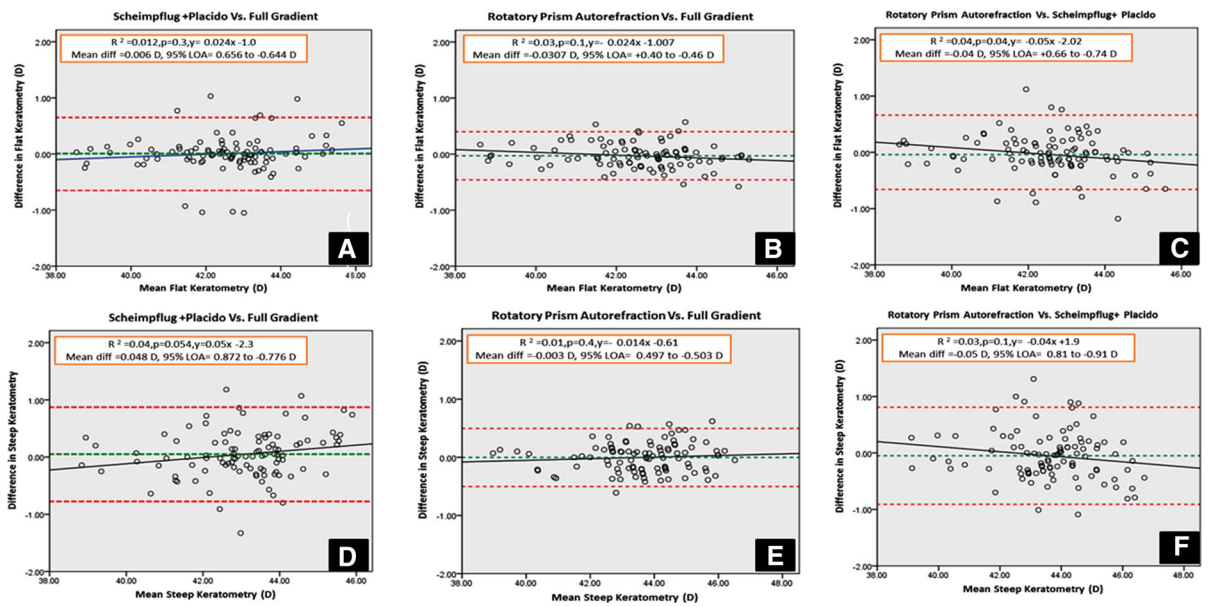

Fig. 5 Bland–Altman plots with difference in the value as a function of the mean of value for two selected variables [Autorefractor (AR), Scheimpflug+Placido (SP), and Hartmann type full gradient topographer (FG)].The *solid line* denotes the linear best fit plot. The *dashed lines* are as follows: uppermost (*red*): upper limit of 95 % LOA, middle (*green*): mean of difference, lowermost (*green*): lower limit of 95 % LOA. **a** flat keratometry for SP versus FG; **b** flat keratometry for AR versus FG; **c** flat keratometry for AR versus SP; **d** steep keratometry for SP versus FG; **e** steep keratometry for AR versus FG; **f** steep keratometry for AR versus SP

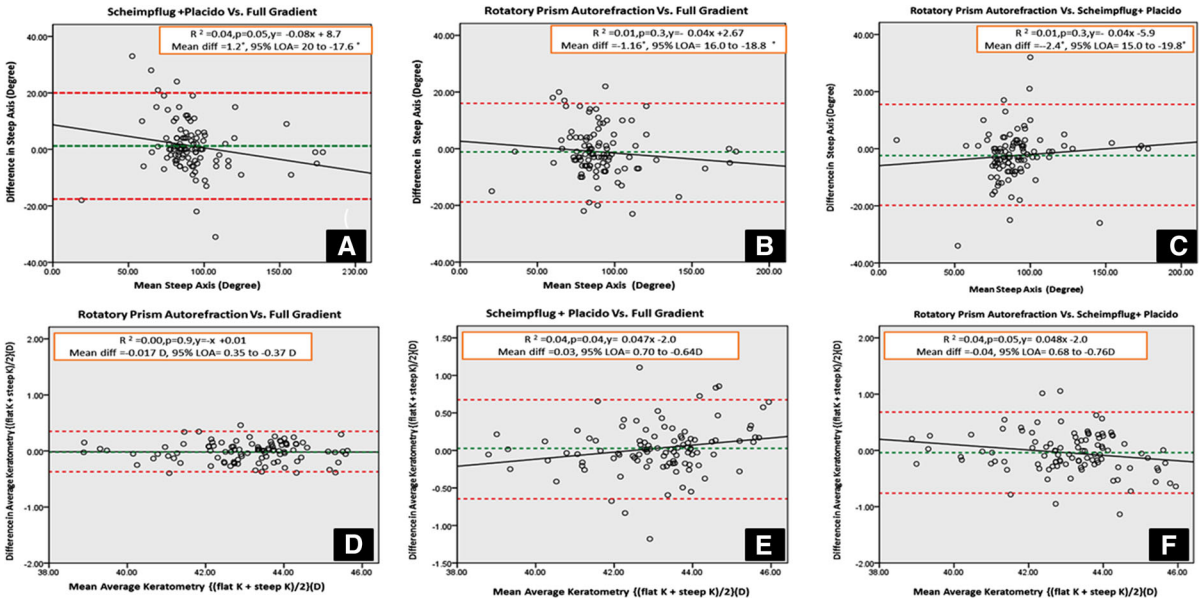

Fig. 6 Bland–Altman plots with difference in the value as a function of the mean of value for two selected variables [Autorefractor (AR), Scheimpflug+Placido (SP), and Hartmann type full gradient topographer (FG)].The *solid line* denotes the linear best fit plot. The *dashed lines* are as follows: uppermost (*red*): upper limit of 95 % LOA, middle (*green*): mean of difference, lowermost (*green*): lower limit of 95 % LOA. **a** steep axis for SP versus FG; **b** steep axis for AR versus FG; **c** steep axis for AR versus SP; **d** average keratometry for SP versus FG; **e** average keratometry for AR versus FG; **f** average keratometry for AR versus SP

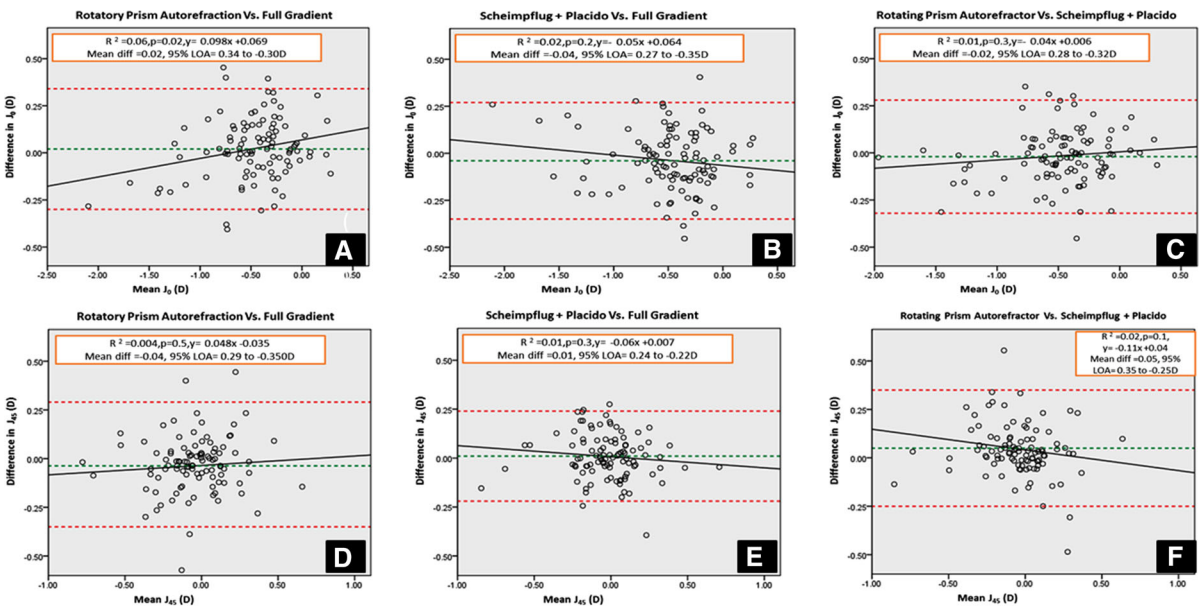

Fig. 7 Bland–Altman plots with difference in the value as a function of the mean of value for two selected variables [Autorefractor (AR), Scheimpflug+Placido (SP), and Hartmann type full gradient topographer (FG)].The *solid line* denotes the linear best fit plot. The *dashed lines* are as follows: uppermost (*red*): upper limit of 95 % LOA, middle (*green*): mean of difference, lowermost (*green*): lower limit of 95 % LOA. **a** J_0 for SP versus FG; **b** J_0 for AR versus FG; **c** J_0 for AR versus SP; **d** J_{45} for SP versus FG; **e** J_{45} for AR versus FG; **f** J_{45} for AR versus SP

We found that the two topographers (iDesign and Sirius) had significantly better repeatability indices compared to the autorefractor-keratometer (KR1). However, the repeatability indices of the two topographers were comparable to each other's.

The Sw versus Average plots showed no significant predictive fits. Therefore, no differences were seen in the intra-device repeatability of the devices over the range of the data studied. This is an important finding in view of the fact that our devices did not have similar repeatability. To offset any inadvertent bias in the outcomes, we randomly selected one measurement from each device for inter-device agreement. All the variables were highly co-related (Figs. 2, 3, 4). Bland–Altman curves showed poor linear fits between the difference and mean, suggesting no systematic change in the difference between the three devices over the range of data studied (Fig. 5, 6, 7). These two factors suggest a possible consistency between the three devices. Even though the devices had good correlation, it would be prudent not to use them interchangeably. The 95 % limits of agreement ranged more than 1 D or more for keratometric parameters. This may lead to potential errors if the devices are used interchangeably for more sensitive calculation such as IOL power calculation and topography derived excimer ablations.

Similar findings have been noted in previous studies comparing corneal power between devices. Crawford, et al. found Orbscan II (Bausch and Lomb, Rochester, NY), Pentcam (Oculus, Wetzlar, Germany), and Galilei (Ziemer Ophthalmic Systems AG, Switzerland) topographers to be sufficiently disparate and recommended that they could not be considered equivalent [3]. Módis L Jr, et al. compared Pentacam, automated kerato refractometry (KR-8100; Topcon, Tokyo, Japan), and corneal topography (TMS-4, Tomey, Erlangen, Germany) [21]. Inspite of high correlation and no significant difference of mean, they recommend that for patient follow-up it would be better to use the same keratometry device. Visser, et al. compared 6 devices and found that Pentacam's equivalent *K* values were not comparable to other keratometers [22].

Therefore, most of the modern devices are repeatable, but not interchangeable for normal eyes. A similar trend of non-interchangeability has been seen by Shetty, et al. even in keratoconic eyes using three devices based on Scheimpflug camera [23]. Therefore, even instruments based on similar principle may not be used to substitute for the other in follow-up monitoring of serial changes.

We found that in our study, there seems to be comparable true data capture from the central 3 mm using the Hartman method with iDesign compared to the Sirius, which compensates for the Placido rings' lack of true central data by Scheimpflug data capture. A further study on comparing the corneal power in post excimer eyes or pathological corneas could provide more information of the comparison of true data captured from Scheimpflug and Hartman type devices in more challenging settings.

In conclusion, we found that in terms of intra-device repeatability, the Hartman Shack-based topographer, iDesign was comparable to the Scheimpflug+Placido-based topographer, Sirius and better than the automated refractor-keratometer, KR1. However, there was satisfactory agreement between the three devices. The high repeatability and low difference in mean values with other commonly used devices ensures that the Hartman Shack type topographer can be used as in clinical practice and decision making in unoperated normal eyes. Even though most comparisons had a low range for limits or agreement range, we recommend against interchanging these devices between serial follow-ups or pooling their data together.

Conflict of interest None of the authors have any financial interests in the products and techniques described in the manuscript and lack thereof.

References

1. Swartz T, Marten L, Wang M (2007) Measuring the cornea: the latest developments in corneal topography. Curr Opin Ophthalmol 18:325–333
2. Oliveira CM, Ribeiro C, Franco S (2011) Corneal imaging with slit-scanning and Scheimpflug imaging techniques. Clin Exp Optom 94:33–42
3. Crawford AZ, Patel DV, McGhee CN (2013) Comparison and repeatability of keratometric and corneal power measurements obtained by Orbscan II, Pentacam, and Galilei corneal tomography systems. Am J Ophthalmol 156:53–60
4. Tajbakhsh Z, Salouti R, Nowroozzadeh MH et al (2012) Comparison of keratometry measurements using the Pentacam HR, the Orbscan IIz, and the TMS-4 topographer. Ophthalmic Physiol Opt 32:539–546
5. Menassa N, Kaufmann C, Goggin M et al (2008) Comparison and reproducibility of corneal thickness and curvature readings obtained by the Galilei and the Orbscan II analysis systems. J Cataract Refract Surg 34:1742–1747

6. Savini G, Carbonelli M, Sbreglia A et al (2011) Comparison of anterior segment measurements by 3 Scheimpflug tomographers and 1 Placido corneal topographer. J Cataract Refract Surg 37:1679–1685
7. Savini G, Barboni P, Carbonelli M, Hoffer KJ (2011) Repeatability of automatic measurements by a new Scheimpflug camera combined with Placido topography. J Cataract Refract Surg 37:1809–1816
8. Miller D, Thall EH, Atebara NH (2004) Ophthalmic Instrumentation. In: Yanoff M, Duker JM (eds) Ophthalmology, 3rd edn. Elsevier, Philadelphia, pp 77–78
9. Klein SA (1997) Corneal topography reconstruction algorithm that avoids the skew ray ambiguity and the skew ray error. Optom Vis Sci 74:945–962
10. Klein SA (1997) Axial curvature and the skew ray error in corneal topography. Optom Vis Sci 74:931–944
11. Savini G, Calossi A, Camellin M et al (2014) Corneal ray tracing versus simulated keratometry for estimating corneal power changes after excimer laser surgery. J Cataract Refract Surg 40:1109–1115
12. Karnowski K, Kaluzny BJ, Szkulmowski M, Gora M, Wojtkowski M (2011) Corneal topography with high-speed swept source OCT in clinical examination. Biomed Opt Express 2:2709–2720
13. Jhanji V, Yang B, Yu M, Ye C, Leung CK (2013) Corneal thickness and elevation measurements using swept-source optical coherence tomography and slit scanning topography in normal and keratoconic eyes. Clin Exp Ophthalmol 41:735–745
14. Mejía Y, Galeano JC (2009) Corneal topographer based on the Hartmann test. Optom Vis Sci 86:370–381
15. Zhou F, Hong X, Miller DT, Thibos LN, Bradley A (2004) Validation of a combined corneal topographer and aberrometer based on Shack-Hartmann wave-front sensing. J Opt Soc Am A Opt Image Sci Vis 21:683–696
16. Stevens JD (2009) Using next-generation topography to screen LASIK candidates. Cataract and Refractive surgery Today Europe. March, 2009. http://bmctoday.net/crstodayeurope/2009/03/article.asp?f=0309_05.php. Accessed 10 Dec 2014
17. Topcon medical systems: KR-1 product brochure. http://www.topconmedical.com/products/kr1-literature.htm. Accessed 10 Dec 2014
18. Thibos LN, Wheeler W, Horner D (1997) Power vectors: an application of Fourier analysis to the description and statistical analysis of refractive error. Optom Vis Sci 74:367–375
19. Bland JM, Altman DG (1996) Measurement error. BMJ 313:744
20. Wang Q, Savini G, Hoffer KJ et al (2012) A comprehensive assessment of the precision and agreement of anterior corneal power measurements obtained using 8 different devices. PLoS One 7:e45607
21. Módis L Jr, Szalai E, Kolozsvári B et al (2012) Keratometry evaluations with the Pentacam high resolution in comparison with the automated keratometry and conventional corneal topography. Cornea 3:36–41
22. Visser N, Berendschot TT, Verbakel F, de Brabander J, Nuijts RM (2012) Comparability and repeatability of corneal astigmatism measurements using different measurement technologies. J Cataract Refract Surg 38:1764–1770
23. Shetty R, Arora V, Jayadev C, Nuijts RM, Kumar M, Puttaiah NK, Kummelil MK (2014) Repeatability and agreement of three Scheimpflug-based imaging systems for measuring anterior segment parameters in keratoconus. Invest Ophthalmol Vis Sci 29:5263–5268